

Short Communication

Dynamic analysis of very flexible beams

R. Fotouhi*

Mechanical Engineering Department, University of Saskatchewan, Saskatoon, Canada S7N 5A9

Received 11 January 2005; received in revised form 12 January 2007; accepted 19 January 2007
Available online 12 June 2007

Abstract

The dynamic analysis of flexible beams with large deformations is difficult and few studies have been performed. In this paper, the vibration analysis of several very flexible beams with large deflections using the finite element approach is studied. The examples were a cantilever beam and rotating flexible robot arms. The results were compared with the results available in the published literature. Several successful checks on the finite element results were performed to ensure the accuracy of the solutions. Due to the geometrical nonlinearity, several static equilibrium shapes can exist for large deflections of a cantilever beam for a given load. Nonlinear dynamic finite element analysis was implemented to investigate the stability of these shapes.

© 2007 Elsevier Ltd. All rights reserved.

1. Introduction

The free vibration problem is of considerable interest to engineers and has been much studied. When the deflections of the structure are small, a wide range of linear analysis tools, such as modal analysis, can be used, and some analytical results are possible. As the deflections become larger, however, geometric (as well as possible material) nonlinearities are introduced which result in effects that are not observed in linear systems. In such situations numerical solution methods must be used. The finite element approach is the most common tool (see Refs. [1–4] for example), however other methods such as the finite difference methods [5–7] have also been considered. In Ref. [7] the transient dynamic motion of a paper sheet emerging from a channel was studied using finite differences in time and space. Within the finite element framework, there are two main issues to consider: geometric nonlinearity and a time stepping algorithm. Numerous ideas have been put forth to deal with the geometric nonlinearities. To date, a popular approach seems to be a co-rotational formulation in which the large motions are considered as small (linear) deformations superimposed on large (nonlinear) rigid body rotations. A linear elastic behavior is typically assumed for the small strains. Most researchers have used some form of Newton's method to deal with the time stepping issues. One approach of interest has been put forth by Simo and Tarnow [8] in which the total energy in the system is used to guide the integration procedure. Some of relevant literatures are quoted below:

*Tel.: +1 306 966 5453; fax: +1 306 966 5427.

E-mail address: reza.fotouhi@usask.ca.

The dynamics of a particular elastica were considered by Snyder and Wilson [9]. The tip rotation angle considered was only about $\pm 15^\circ$, which is not very large compared to the examples discussed in this paper. A finite element method employing element-fixed moving reference frames was used in Ref. [10] to analyze flexible beams undergoing large and fast rotations; the authors compared their results against those obtained using the commercial package ABAQUS and concluded that their approach worked while those of ABAQUS failed to converge. They also reported that the commercial FEM software NASTRAN failed to predict the correct maximum deflection for membrane stiffness dominated problems. These statements are interesting in lieu of the fact that in this paper the ability of ANSYS, a commercial FE software, for handling similar problems is discussed. The dynamics of flexible beams that have undergone large overall motions (spin-up maneuvers) with small elastic deformations using a closed form nonlinear approach was presented in Ref. [11]. A finite element analysis of a rotating flexible cantilever beam was given in Ref. [12]. This approach is very similar to Ref. [11], but uses finite elements instead of closed form dynamics. However, in solved examples, the deformations of the beam with respect to shadow beam were relatively small. A finite element modeling of the dynamics of flexible multi-body systems was considered in Ref. [13]. Numerical examples for systems undergoing large overall motion were solved using constant and energy decaying approaches in Ref. [8]. A nonlinear finite element model for the dynamic analysis of flexible linkages was presented in Ref. [14]. The linkage modeled as a beam had large rigid body motion and elastic small deformation. An experimental investigation into the nonlinear dynamics of a flexible cantilevered rod (elastica) was discussed in Ref. [15]. However, from numerical examples given in the paper, it is not clear how large were the deformations. In a later paper [16], the authors derived a model for the study of the vibration of the thin elastica based on experimental observation. A non-incremental finite element formulation for large rotation/deformation of flexible bodies was developed in Ref. [17]. It involved a transient dynamic loading problem. A numerical approach for the study of large deformations of nonlinear elastic rods using the theory of a Cosserat point, for static equilibrium of elastica, was given in Ref. [18]. A finite element analysis of rotating beams (large rigid body rotation with small deformation) was reported in Ref. [19]. A flexible multi-body dynamic formulation was considered in Ref. [20].

The main differences of the above works and that reported in this paper is allowing much larger deflections (large amplitude vibration) of flexible beams and the use of finite element analysis. The object of the present work was to investigate the nonlinear free vibration problem of a uniform cantilever beam undergoing very large deflections. Specifically, the goals of this study were as follows. The first goal was to detail the behavior of the problem as it transforms from a linear to a nonlinear problem. The second goal arose from the fact that while some authors (such as those mentioned above) develop finite element code to implement their particular approach to similar problems, what seems to be missing from the literature is an evaluation of the ability of common commercial finite element packages to accurately consider the large deformation problems. For this reason the study of the large deflection vibration problem using the finite element package ANSYS was undertaken. Of particular interest in this regard was the accuracy and stability of the solution procedure, as well as the solution time requirements. The third and final goal was the investigation of the stability of particular equilibrium positions using a full nonlinear dynamic analysis.

2. Numerical approach—finite element method

The dynamics of flexible bodies can be simulated by using the finite element method (FEM), which is the most common of the numerical approaches available for solving geometric nonlinearities.

2.1. Solution procedure

The object is to investigate the nonlinear vibration problem of a uniform cantilever beam undergoing very large deflection. The motion of flexible beam is simulated by using the ANSYS Finite Element program, which solves the problem by direct integration of the nonlinear equations of motion. Transient dynamic analysis used here, is a technique used to determine the dynamic response of a flexible structure under the action of any general time-dependent load. This analysis can be used to determine the time-varying displacements, strains, stresses and forces in a structure due to any static, transient, and harmonic load.

The equations of motion, solved by a transient dynamic analysis, can be written in the following form:

$$M(x)\ddot{x}(t) + C(x)\dot{x}(t) + K(x)x(t) = u(t),$$

where $M(x)$, $C(x)$, and $K(x)$ are geometry dependent mass, damping, and stiffness matrices, and x , \dot{x} , \ddot{x} are vectors of nodal displacement (degrees of freedom (dof)), nodal velocity, and nodal acceleration, respectively; and $u(t)$ is the vector of external loads driving the system. In ANSYS three methods are available to carry out a transient dynamic analysis: full, reduced, and mode superposition. Details are given in Appendix A. In this paper, the full transient dynamic analysis was used due to presence of geometric large deflections. A transient dynamic analysis involves three steps, building the model, applying loads and obtaining the solution, and reviewing the results.

A two-dimensional elastic beam element (BEAM3) was used to model the flexible structure. The beam section was considered rectangular. For all of the examples given here, 50 BEAM3 elements were used. Fifty was the optimum number of elements chosen from the cases where 10–200 elements were investigated. This was a compromise between accuracy and computational time. The matrices M , C , and K are constant for elements when defined in the local coordinate system. However they become functions of the dof when assembling the elements in the global coordinate system due to geometric nonlinearities. The stiffness changes because the shape changes or the body rotates. It is notable that the program creates a geometric stiffness matrix, K_G , for geometric nonlinearity. This matrix is added to the regular stiffness matrix, K , and is updated every several iterations such that $M\ddot{x} + C\dot{x} + (K + K_G)x = u$. The updated stiffness matrix represents the correct deformed configuration of the system. The first step in applying transient loads was to establish initial conditions. To apply initial conditions, a static analysis was performed to transfer the system from a straight horizontal position to the initial condition (equilibrium positions 1, 2, or 3) to start the vibration analysis. This was achieved by applying a static load at the tip of the beam when transient effect was off. This load was applied in four steps (so that the program could converge to the desired equilibrium position when stress stiffening effect was on) due to very large deflection of the beam.

3. Validation

The problems considered here were conservative (during the entire or part of the motion); thus one important check was to monitor the consistency of the total mechanical energy of the system. The effect of parameters such as time step on this behavior was considered. Other checks for specific problems will be discussed at the appropriate point in the text. One of the method used here to validate ANSYS for this particular type of analysis was to compare the result generated here with the examples in published literature. Three examples were used. These examples were also used in Refs. [21–23].

3.1. Example 1

The first example is a displacement driven flexible robot arm, which is a simple case of spin-up maneuver (Example 2.1.1 of Ref. [21]). The same problem was solved in Refs. [22,23]. This flexible robot arm rotates horizontally about a vertical axis which passes through base of the arm. For this example, fifty BEAM3 elements were used (50 is the optimum number of elements). For simulation, the following parameters were used: beam length $L = 10.0$ in (0.254 m), modulus of elasticity $E = 40.0E3$ psi (0.276 Gpa), beam cross section $A = 0.250$ in² ($1.61E - 4$ m²), area moment of inertia of beam $I = 0.025$ in⁴ ($1.04E - 8$ m⁴), and density $\rho = 5.40$ lb s²/in⁴ (57.7 Gg/m³) such that $EA = 10.0E3$ lb (44.5 kN) and $EI = 1.00E3$ lb in² (2.87 N m²) as in Ref. [21]. The rotation angle of the base, θ_Z , was changed linearly from 0 to 1.5 rad in 5 s. The base rotation angle stayed constant, 1.5 rad, for time $t \geq 5$. The arm position is shown in ten equal intervals during this period in Fig. 1. Once the angle was fixed, the robot arm underwent free vibration. These results comply closely with those in Refs. [21] (see Fig. 11), [22,23]. The total mechanical energy (TE) of the beam during the free vibration phase ($5 \leq t \leq 10$ s) should be constant. As can be seen in Fig. 2, this total energy was almost constant with a drop of about 0.02% over 5 s; i.e. 0.004% per second. Tip forces were another check on accuracy of the results. These forces (not shown here) should be zero, and they almost were zero. The small amount of forces present were due to the fact that BEAM3 is a constant strain element (see Eq. (A.1) in Appendix A).

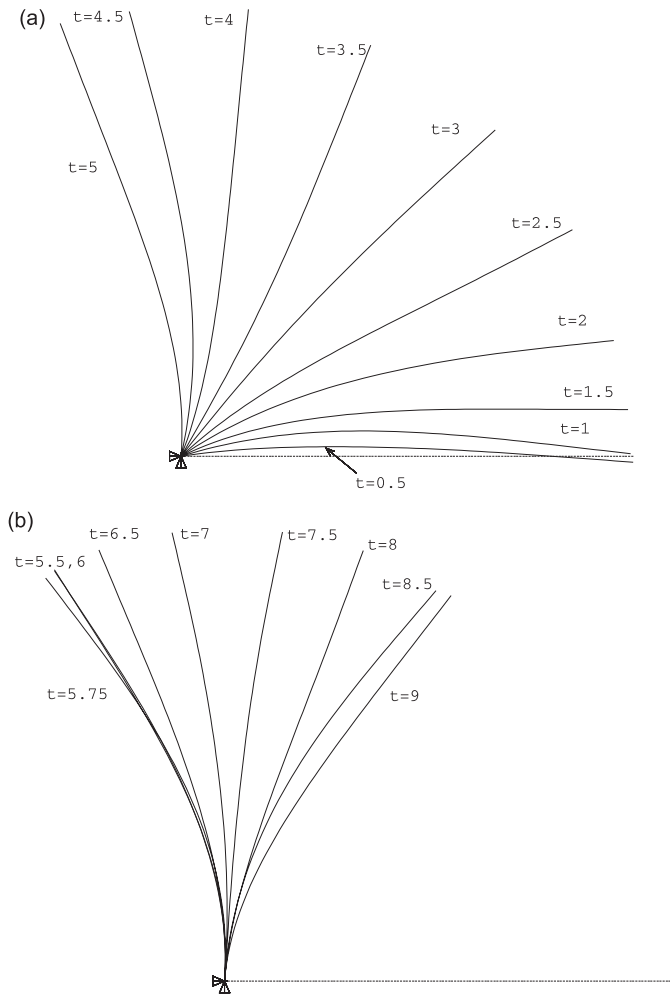


Fig. 1. Example 1, rotation of arm: (a) from 0.5 to 5 s, (b) from 5.5 to 9 s.

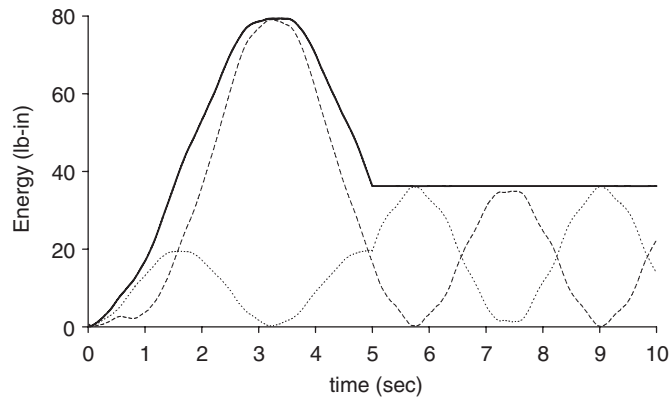


Fig. 2. Example 1, mechanical energy of the arm for $0 \leq t \leq 10$ s. solid: total, dashed: kinetic, dotted: strain, total energy at $t = 5$ is 36.25 and at $t = 10$ is 36.24.

3.2. Example 2

The second example is a force driven robot arm (Example 2.1.2 of Ref. [21]) and also solved in Ref. [23]. The flexible robot arm is driven horizontally about base of the arm. A constant torque of $\tau_o = 80.0 \text{ lb in}$ (9.10 N m) was applied to the base of arm for $0 \leq t < 2.5 \text{ s}$ and removed instantly; the robot then moved freely afterward $t \geq 2.50$. As before, fifty BEAM3 elements were used. For simulation, the parameters used were the same as those in Example 1 and as in Ref. [21]. The arm position in five equal intervals in 2.50 s is shown in Fig. 3. The applied torque was removed at $t = 2.50$, and the robot arm underwent a free rotation as shown also in 25 equal intervals in Fig. 3. These results comply closely with those in Refs. [21] (see Fig. 11) and [23]. Total mechanical energy of the beam during free rotation phase ($2.5 \leq t \leq 15 \text{ s}$) should be constant. As shown in Fig. 4, this total energy was almost constant with a drop of about 2% over 12.5 s or 0.16% per second. The variation of total energy here was a little bigger than that of example one. This can be attributed to the fact that the arm underwent a much larger rotation than before and subsequently numerical error became larger. Again, tip forces (not shown here) should be zero, which they almost were zero.

3.3. Example 3

The third example is a similar beam as in example 1, however, it is now subject to a given spin-up maneuver (Example 2.4 of Ref. [21]). It is not as simple case as Example 1. The same problem was solved in Ref. [10]. For this example, again 50 BEAM3 elements were used. For simulation, the following parameters were used: beam length $L = 10 \text{ in}$ (0.254 m), modulus of elasticity $E = 1.12E8 \text{ psi}$ (772 Gpa), beam cross section $A = 0.250 \text{ in}^2$ ($1.61E-4 \text{ m}^2$), area moment of inertia of beam $I = 0.125E-3 \text{ in}^4$ ($5.20E-11 \text{ m}^4$), and density $\rho = 4.80 \text{ lbs}^2/\text{in}^4$ ($51.3 \text{ Gg}/\text{m}^3$) such that $EA = 2.80E7 \text{ lb}$ ($1.24E5 \text{ kN}$), $EI = 1.40E4 \text{ lb in}^2$ (40.2 N m^2), $A\rho = A \cdot \rho = 1.20 \text{ lbs}^2/\text{in}^2$ ($8.26 \text{ Mg}/\text{m}$), and $I\rho = I \cdot \rho = 6.00E-4 \text{ lbs}^2$ ($0.267E-2 \text{ kg m}$) as in Ref. [21]. The rotation angle of base, θ_Z , is given as

$$\theta_Z(t) = \left\{ \begin{array}{ll} \frac{6}{15} \left[\frac{t^2}{2} + \left(\frac{15}{2\pi} \right)^2 \left(\cos \frac{2\pi t}{15} - 1 \right) \right] \text{ rad} & 0 \leq t < 15 \text{ s} \\ (6t - 45) \text{ rad} & t \geq 15 \text{ s} \end{array} \right\}.$$

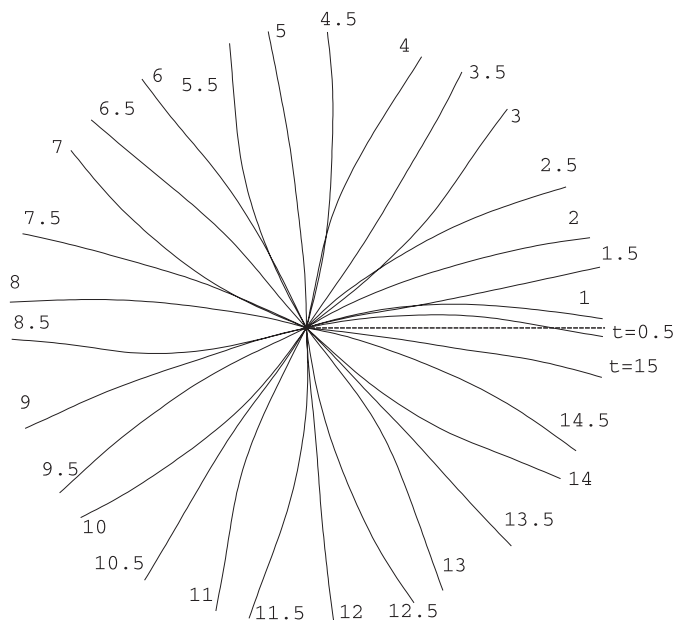


Fig. 3. Example 2, rotation of arm, from 0.5 to 15 s

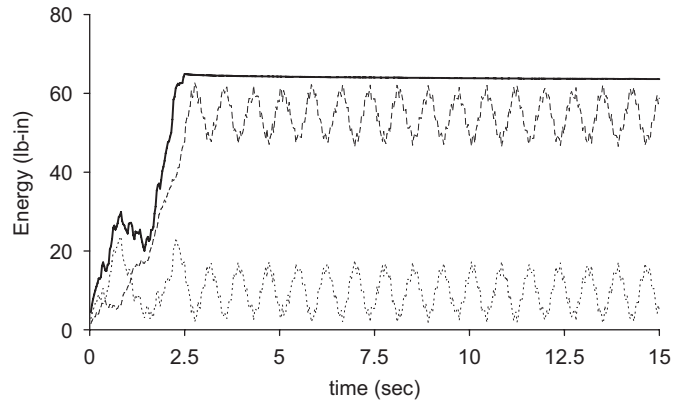


Fig. 4. Example 2, mechanical energy of the arm for $0 \leq t \leq 15$ s. Solid: total, dashed: kinetic, dotted: strain. Total energy at $t = 2.5$ is 64.93 and at $t = 15$ is 63.62.

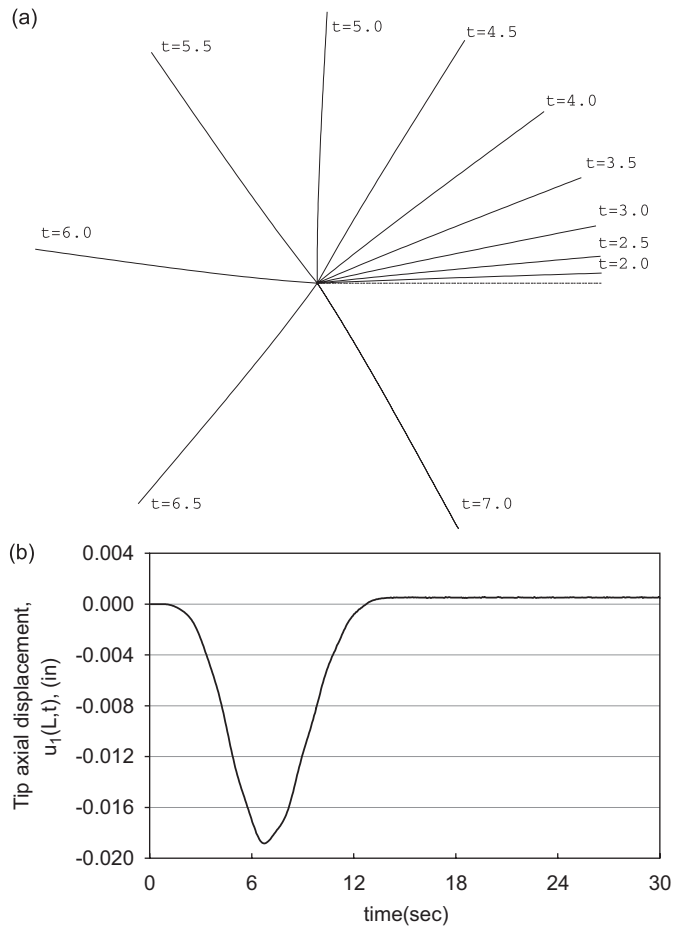


Fig. 5. Example 3, (a) rotation of the arm from 0 to 7 s, (b) tip axial relative displacement of the arm.

The results obtained comply closely with those in Refs. [21,10] (compare Fig. 5 with Fig. 12). The displacements shown here are relative displacements (with respect to shadow, or rigid, beam) to be able to compare them with those of Ref. [21].

4. Large amplitude free vibration of cantilever beams

As it was said earlier the free vibration problem is of considerable interest to engineers. The object of the present work is to investigate the nonlinear free vibration of a uniform cantilever beam released from rest after having undergone very large deflections initially due to a static transverse load.

4.1. Problem solution

A cantilever straight beam with a uniform rectangular cross section in horizontal plane was considered. To apply initial condition for transient dynamic analysis, a large lateral load was applied to the tip of the beam statically (time integration effect was off). It was necessary to set a very small time to perform this step. A non-dimensional load was defined as $\alpha = \sqrt{PL^2/EI}$ where P is the lateral load, L is the length of the beam and EI is the flexural rigidity of the beam. A load factor of $\alpha = 5.0$ was considered here which resulted initially in a very large deflection. Once the initial displacement was determined, the static load was removed and the transient dynamic analysis was started. For simulation, the following parameters were used: Beam's length $L = 100$ in (2.54 m), modulus of elasticity $E = 3.00E7$ psi (207 Gpa), beam's rectangular cross section $A = H^2 = 0.250$ in² ($1.61E-4$ m²) in which H is height of the beam, area moment of inertia of beam $I = H^4/12 = 5.21E-3$ in⁴ ($2.17E-9$ m⁴), and density of the steel beam was set to $\rho = 7.35E-4$ lb s²/in⁴ ($7.85E3$ kg/m³). This load ($\alpha = 5.0$, corresponds to $P = 391$ lb (1.74 kN)) has three *equilibrium shapes or positions* (see Ref. [24]), here referred to as shape 1, shape 2 and shape 3 (see Fig. 6). Fifty BEAM3 element were used for equilibrium position one, and 60 for positions two and three. The equilibrium positions 1, 2, and 3 were used as initial conditions for transient dynamic analysis. These equilibrium positions were obtained by applying specific loading patterns in the static analyzes.

4.2. Finite element analysis results

In Figs. 7 and 8 are shown the deflected shape of the beam at selected times in the first cycle of the vibration as initiated from the equilibrium positions 1 and 3, respectively. The vibration of the beam initiated from , shape 2 was chaotic, as discussed later. Shown in Figs. 9 and 10 are the kinetic, strain and *conservation of total*

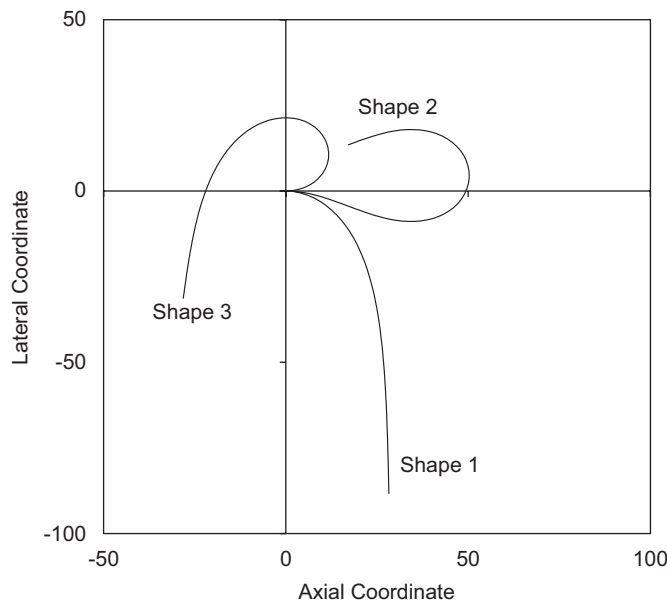


Fig. 6. Three equilibrium shapes of a cantilever beam corresponding to $\alpha = 5.0$.

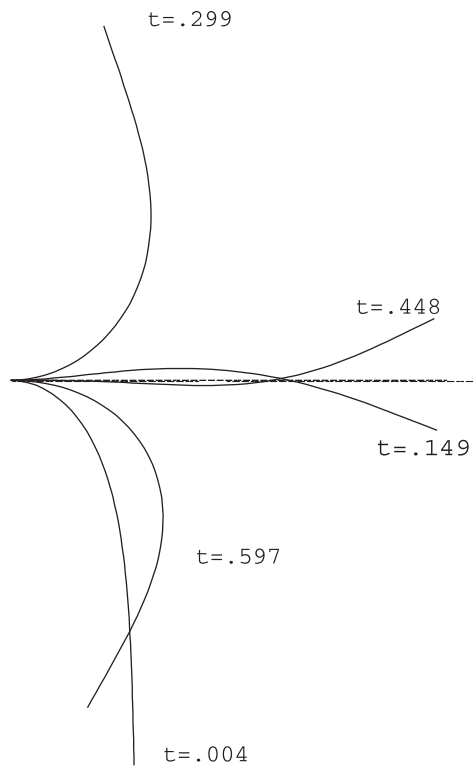


Fig. 7. Deflected shape of a cantilever beam at selected times in one cycle of vibration started from equilibrium shape 1 corresponding to $\alpha = 5.0$.

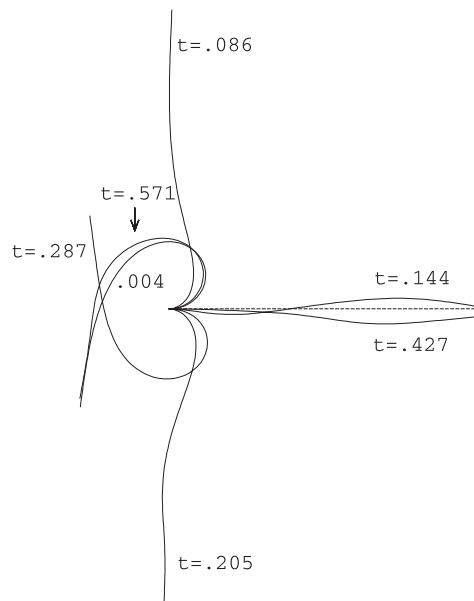


Fig. 8. Deflected shape of a cantilever beam at selected times in one cycle of vibration started from equilibrium shape 3 corresponding to $\alpha = 5.0$.

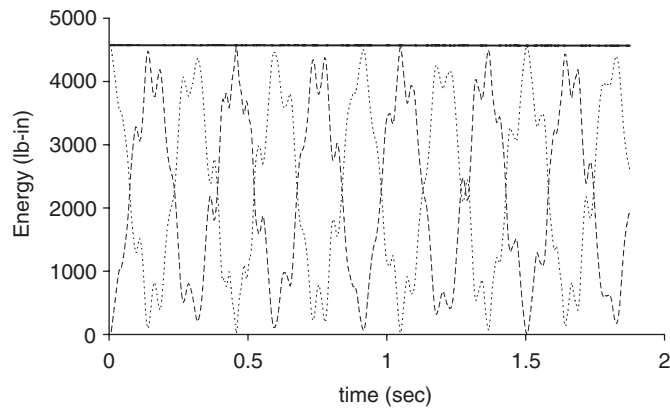


Fig. 9. Mechanical energy of a cantilever beam in three cycles of vibration started from equilibrium shape 1 corresponding to $\alpha = 5.0$. Solid: total, dashed: kinetic, dotted: strain. Total energy at $t = .0037$ is 4576 and at $t = 1.875$ is 4567.

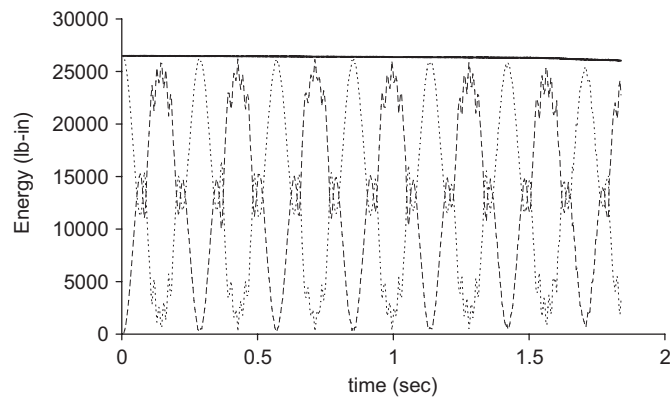


Fig. 10. Mechanical energy of a cantilever beam in three cycles of vibration started from equilibrium shape 3 corresponding to $\alpha = 5.0$. Solid: total, dashed: kinetic, dotted: strain. Total energy at $t = .0036$ is 26481 and at $t = 1.838$ is 26034.

mechanical energy of the beam as a function of time in three cycles initiated from equilibrium positions 1 and 3, respectively. As can be seen from the figures, the total mechanical energy were almost constant for these two cases. The variations of total energy were .19% in about 2 s (.01% per second) for position 1, and 1.7% in about 2 s (.92% per second) for position 3 for three cycles of vibration; for position 2 this drop was .013% in about 0.2 s (not shown here). As time increased the drop of total energy became larger for equilibrium position 2 (see related discussion on stability, in the next section, for this shape).

Note that while ideally the energy loss should be zero for this conservative problem, the nature of this problem is such that it is exceedingly difficult to obtain a constant energy level. A careful observation of the total energy shows that for some cases a significant portion of the energy loss occurs during the very first part of the motion. This pattern is most easily explained if one considers the boundary conditions at the free end of the beam. In the initial configuration, which is obtained as the static equilibrium solution for an applied tip load, the tip of the beam is not a “free-end”, but rather there is an applied shear load there. As a result at the tip of beam $d^2\theta_z/ds^2 \neq 0$. Shortly after the load is removed, the tip becomes a free end and $d^2\theta_z/ds^2 = 0$. It is the propagation and reflection of axial waves which governs the transition between these two states. In order to have any possibility of observing this transition clearly, not only would different elements with more freedom in the axial direction be required, but it would also be necessary to use very small time steps to capture details of the axial waves (which occur at significantly higher frequencies than the lateral vibration). This would be prohibitively expensive computationally and is not the goal of the present work. As a result we

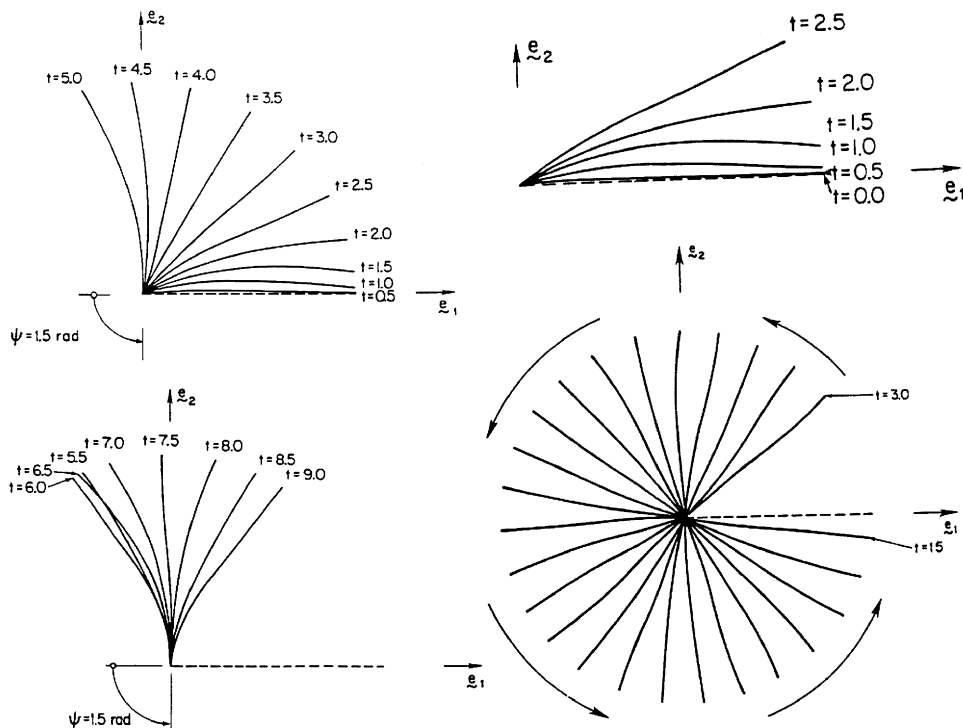


Fig. 11. Examples 1 and 2, Simo's results [21] for comparison with Figs. 1 and 3. (Reproduced from Simo, J.C. and Vu-Quoc, L., ASME Journal of Applied Mechanics 53, 855–863 (1986) with permission).

are missing out on the fine detail of the solution at early stages in favor of the long term response of the structure. In light of these ideas, the small amounts of energy loss observed in the solutions seems quite acceptable. Note that these ideas also play a role in the purely linear (small deflection) situation where the geometric nonlinearities do not play a role. Even in the linear situation (not shown), it can be observed that the energy loss occurs almost entirely in the first small part of the motion, similar to the results observed in the large deflection case discussed above.

4.3. Stability analysis

The use of a finite element formulation to evaluate the stability of geometrically nonlinear equilibrium configurations will now be considered for the three equilibrium shapes shown in Fig. 6 corresponding to $\alpha = 5.0$. The same finite element models as discussed in Section 4.1 are used here as well. The basic approach used to investigate the stability was to introduce perturbations to the equilibrium configuration and to determine the subsequent motion of the structure. If the subsequent motions remained small, the configuration was considered stable, but if the perturbation grew larger, the equilibrium position was unstable. The specific perturbations used in the current work are described below. In order to introduce perturbation to the equilibrium shapes shown in Fig. 6, the following procedure was used. Initially, an equilibrium configuration was determined which corresponded to the applied load $\alpha = 5.0$ plus a small additional load at the beam's tip. Once this equilibrium position was established, the small additional load was then removed and the full dynamic analysis was started. In this way, the beam was started in a slightly perturbed configuration, which was very close to the equilibrium shapes shown in Fig. 6. It should be noted that this was a preliminary stability analysis, not a comprehensive one (where the magnitude and/or direction of the perturbed load are considered unknown variables). In the present work, the tip load used corresponded approximately to a change in α of ± 0.01 in both the vertical and horizontal directions. That is, two of the perturbed positions

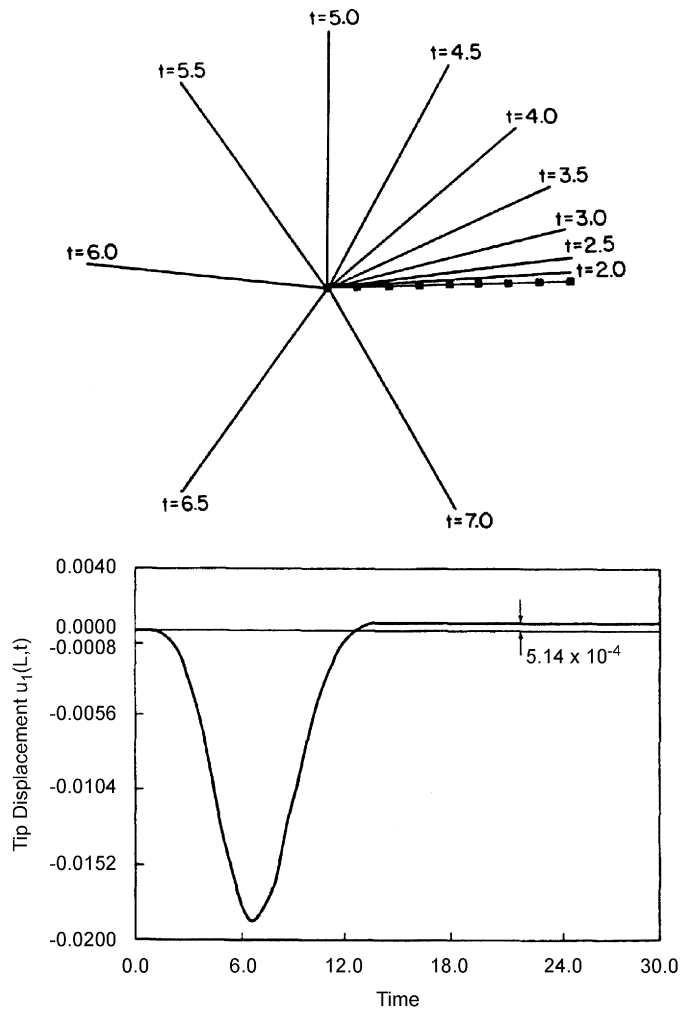


Fig. 12. Example 3, Simo's results [21] for comparison with Fig. 5. (Reproduced from Simo, J.C. and Vu-Quoc, L., ASME Journal of Applied Mechanics 53, 855–863 (1986) with permission).

considered included equilibrium shapes corresponding to $\alpha = 4.99$ and 5.01 . Similarly, the other two perturbed configurations considered were equilibrium shapes corresponding to $\alpha = 5.00$ plus a small additional load in both the positive and negative horizontal directions.

Shape 1 was found to be stable for all of the applied perturbation loads. The dynamic equations predicted small oscillatory motions about the equilibrium configuration. The frequency of these small motions (as estimated from a plot of the tip deflection in the axial s and lateral y directions) agreed well with the natural frequencies for pre-stressed large deflection eigenvalue analysis as predicted by ANSYS. Very similar results were obtained for shape 3, which was found to be stable for all of the perturbation loads considered. Again, the frequencies of the motions agreed well with those predicted by a pre-stressed large deflection eigenvalue analysis of shape 3. Shape 2 however, was found to be unstable. Any of the applied perturbation loads caused large motions which caused the beam to “flop” towards either shape 1 or 3, depending on the direction of the perturbation. Qualitatively, these results were fairly intuitive and agreed well with previously published results [24] for this load ($\alpha = 5$). In all of the cases considered above, the total energy of the system was monitored as a check on the accuracy of the solution. The energy was conserved to within approximately 1–2% (except for the shape 2 which was more); in all these cases the largest changes in total energy occurred for shape 2 as the motions became large.

5. Conclusions

The geometrically nonlinear, large amplitude vibration of several very flexible beams predicted by using the finite element (FE) package ANSYS was analyzed. The FE responses of the systems were compared with the responses of similar models available in published works. Very good agreement was observed for the three examples examined. Also several successful checks on the FE results were performed to ensure the accuracy of the solution. It was shown that finite element analysis is a reliable approach and can produce acceptable (good) results for the large amplitude vibration analysis of very flexible beams. It is sometimes much more economical and easier to use these commercial FE codes, if they have been independently verified for the particular analysis, than developing one's own code. Due to the geometric nonlinearity (large deflections), several static equilibrium shapes can exist for the elastica of a given load. An investigation of the dynamic stability with large deflection was performed for some of these shapes. Evaluation of other FE software, such as ADINA, for such a problem is underway and the results will be published when available.

Acknowledgements

The financial support from a NSERC discovery grant is acknowledged, as are the contributions of Dr. Don Raboud and Dr. Bill Lipsett for their fruitful discussions pertaining to the work described in this paper. Also contribution of Dr. Peter N. Nikiforuk in editing the manuscript is acknowledged.

Appendix A. ANSYS details

The ANSYS program uses the Newmark time integration method to solve equations of motion in time. The time increment between successive time-points is called the integration time step. The natural frequencies of the system are used for calculating the correct integration time step. In ANSYS three methods are available to do a transient dynamic analysis: full, reduced, and mode superposition. The full method uses the full system matrices to calculate the transient response; that is there is no matrix reduction as in the reduced method. It is most powerful of the three methods because it also allows all types of nonlinearities to be included (plasticity, large deflection, and large strain, etc.) However, it is computationally the most expensive method of the three. In the reduced and mode superposition methods, the nonlinearity due to large deflection is not allowed. In this paper, the full transient dynamic analysis was used due to presence of geometric large deflections. Doing a transient dynamic analysis involved three steps, building the model, applying the loads and obtaining the solution, and reviewing the results.

A.1. Model used: number and type of elements, and solver

The two-dimensional elastic beam element (BEAM3) of the ANSYS element library was used here to model the flexible structure. The element has three dof at each of its two nodes: translations in the local axial s and lateral y directions and rotation about the nodal z -axis (perpendicular to s and y in a right-hand coordinate system.) The shape functions for this element are linear in the s direction and the third-order polynomial in the y direction as follows:

$$u = \frac{1}{2}(u_I(1-s) + u_J(1+s)), \quad -1 \leq s \leq 1, \quad (\text{A.1})$$

$$v = \frac{1}{2} \left[v_I \left(1 - \frac{s}{2} (3 - s^2) \right) + v_J \left(1 + \frac{s}{2} (3 - s^2) \right) \right] + \frac{L}{8} [\theta_{zI}(1-s^2)(1-s) + \theta_{zJ}(1-s^2)(1+s)], \quad (\text{A.2})$$

where L is the length of the element, and θ_z represents rotation about the z -axis. Here u and v are displacements in the s and y directions, respectively, and u_I and v_I represent these displacements in the node I . Options used in transient dynamic analysis are as follows: transient dynamic analysis (TRNOPT, FULL):

full method was used, large deformation effects (NLGEOM,ON): for large deflections and large geometric nonlinearities, Stress stiffening effects (SSTIF,ON): for convergence in a large deflection analysis, Newton–Raphson option (NROPT,FULL,ON): full Newton–Raphson with adaptive decent on (this option specifies how often the tangent matrix is updated during solution and was used here because nonlinearities were present), Equation solver option (EQSLV,SPARSE): default when “solcontrol” is on (ANSYS offers eight different solver; SPARSE solver worked best in here for geometric nonlinearities). Integration time step (DELTIM) is the time increment used in the time integration of equations of motion. The size of time step determines the accuracy of the solution. The smaller its value, the higher the accuracy. The initial time step used was inverse of the fundamental natural frequency (period) divided by (512×20) . Automatic time stepping was on (AUTOTS,ON): This option, also known as time-step optimization in a transient analysis, increases or decreases the integration time step based on the response of the structure. Nonlinear options used: Maximum number of equilibrium iterations (NEQIT,250), Convergence Tolerance (CNVTOL) was 10^{-5} .

References

- [1] I. Fried, Stability and equilibrium of the straight and curved elastica-finite element computation, *Computer Methods in Applied Mechanics and Engineering* 28 (1981) 49–61.
- [2] R.F. Gans, On the dynamics of a conservative elastic pendulum, *ASME Journal of Applied Mechanics* 59 (1992) 425–430.
- [3] M. Stylianou, B. Tabarrok, Finite element analysis of an axially moving beam, part i: time integration, *Journal of Sound and Vibration* 178 (1994) 433–453.
- [4] M. Stylianou, B. Tabarrok, Finite element analysis of an axially moving beam, part ii: stability analysis, *Journal of Sound and Vibration* 178 (1994) 455–481.
- [5] B.D. Coleman, J.-M. Xu, On the interaction of solitary waves of flexure in elastic rods, *Acta Mechanica* 110 (1995) 173–182.
- [6] S. Essebie, G. Baker, Computational techniques for nonlinear dynamics of continuous systems, *Journal of Engineering Mechanics* 121 (1995) 1193–1199.
- [7] J. Stolte, R.C. Benson, Dynamic deflection of paper emerging from a channel, *Journal of Vibration and Acoustics* 114 (1992) 187–193.
- [8] J.C. Simo, N. Tarnow, Non-linear dynamics of three-dimensional rods: exact energy and momentum conserving algorithms, *International Journal for Numerical Methods in Engineering* 38 (1995) 1431–1473.
- [9] J.M. Snyder, J.F. Wilson, Dynamics of the elastica with end mass and follower loading, *ASME Journal of Applied Mechanics* 57 (1990) 203–208.
- [10] T.Y. Tsang, A. Arabyan, A novel approach to the dynamic analysis of highly deformable bodies, *Computers and Structures* 58 (1996) 155–172.
- [11] H.H. Yoo, R.R. Ryan, R.A. Scott, Dynamics of flexible beams undergoing overall motions, *Journal of Sound and Vibration* 181 (1995) 261–278.
- [12] J. Chung, H.H. Yoo, Dynamic analysis of a rotating cantilever beam by using the finite element method, *Journal of Sound and Vibration* 249 (2002) 147–164.
- [13] A. Ibrahimbegovic, R.L. Taylor, H. Lim, Non-linear dynamics of flexible multibody systems, *Computers and Structures* 81 (2003) 1113–1132.
- [14] H. Du, S.F. Ling, A nonlinear dynamics model for three-dimensional flexible linkages, *Computers and Structures* 56 (1995) 15–23.
- [15] J.P. Cusmano, F.C. Moon, Chaotic non-planar vibrations of the thin elastica, part i: experimental observation of planar instability, *Journal of Sound and Vibration* 179 (1995) 185–208.
- [16] J.P. Cusmano, F.C. Moon, Chaotic non-planar vibrations of the thin elastica, part ii: derivation and analysis of a low-dimensional model, *Journal of Sound and Vibration* 179 (1995) 209–226.
- [17] A.A. Shabana, H.A. Hussien, J.L. Escalona, Application of the absolute nodal coordinate formulation to large rotation and large deformation problems, *Journal of Mechanical Design, Transactions of the ASME* 120 (1998) 188–195.
- [18] M.B. Rubin, Numerical solution procedures for nonlinear elastic rods using the theory of a cosserat point, *International Journal of Solids and Structures* 38 (2001) 4395–4437.
- [19] J.J. Jiang, C.L. Hsiao, A.A. Shabana, Calculation of non-linear vibration of rotating beams by using tetrahedral and solid finite elements, *Journal of Sound and Vibration* 148 (1991) 193–213.
- [20] J.A.C. Ambrosio, Dynamics of structures undergoing gross motion and nonlinear deformations: a multibody approach, *Computers and Structures* 59 (1996) 1001–1012.
- [21] J.C. Simo, L. Vu-Quoc, On the dynamics of flexible beams under large overall motions-the plane case: part ii, *ASME Journal of Applied Mechanics* 53 (1986) 855–863.
- [22] K.-M. Hsiao, J.-Y. Jang, Dynamic analysis of planar flexible mechanisms by co-rotational formulation, *Computer Methods in Applied Mechanics and Engineering* 87 (1991) 1–14.
- [23] J.L. Meek, H. Liu, Nonlinear dynamics analysis of flexible beams under large overall motions and the flexible manipulator simulation, *Journal of Computers and Structures* 56 (1995) 1–14.
- [24] D.W. Raboud, A.W. Lipsett, M.G. Faulkner, J. Diep, Stability evaluation of very flexible cantilever beams, *International Journal of Non-Linear Mechanics* 37 (2001) 1109–1122.